# Eisosomes are metabolically regulated storage compartments for APC-type nutrient transporters

Akshay Moharir[a], Lincoln Gay[a], Daniel Appadurai[a], James Keener[b], and Markus Babst[a,*]
[a]Henry Eyring Center for Cell and Genome Science and [b]Department of Mathematics, University of Utah, Salt Lake City, UT 84112

**ABSTRACT** **Eisosomes are lipid domains of the yeast plasma membrane that share similarities to caveolae of higher eukaryotes. Eisosomes harbor APC-type nutrient transporters for reasons that are poorly understood. Our analyses support the model that eisosomes function as storage compartments, keeping APC transporters in a stable, inactive state. By regulating eisosomes, yeast is able to balance the number of proton-driven APC transporters with the proton-pumping activity of Pma1, thereby maintaining the plasma membrane proton gradient. Environmental or metabolic changes that disrupt the proton gradient cause the rapid restructuring of eisosomes and results in the removal of the APC transporters from the cell surface. Furthermore, we show evidence that eisosomes require the presence of APC transporters, suggesting that regulating activity of nutrient transporters is a major function of eisosomes.**

**Monitoring Editor**
Thomas D. Fox
Cornell University

Received: Nov 30, 2017
Revised: Jun 11, 2018
Accepted: Jun 13, 2018

## INTRODUCTION

It is well established that cellular membranes, in particular the plasma membrane, are subdivided into domains with discrete functions. These lipid–protein microdomains are highly dynamic and usually too small to observe by conventional fluorescence microscopy, which limits the ability to study these structures. However, in the yeast *Saccharomyces cerevisiae* large plasma membrane furrows have been identified (~50 nm deep, ~500 nm long) that are enriched in sphingolipids, ergosterol, and a set of transmembrane proteins, namely, the tetraspans Nce102, Sur7, and the nutrient transporters Can1, Tat2, and Fur4. Furthermore, the membrane-associated, BAR domain–containing proteins Pil1, Lsp1, and Slm1/2 have been localized to these membrane domains. Because of the curved, elongated structure of the BAR domains it has been proposed that these proteins are in part responsible for shaping the plasma membrane into the observed furrows (reviewed in Douglas and Konopka, 2014). Originally, the lipid domain and the membrane-associated BAR domain proteins were identified separately, with the lipid domain named MCC (Membrane Compartment of Can1; Malinska *et al.*, 2003) and the membrane-associated protein complex called eisosome. However, in later studies it became clear that these two structures were in fact parts of the same structure, which we refer to as eisosomes (Walther *et al.*, 2006).

Eisosomes have been shown to function in the regulation of sphingolipid synthesis and in the response to plasma membrane stress (Frohlich *et al.*, 2009; Kamble *et al.*, 2011; Berchtold *et al.*, 2012). Mechanical stress or low sphingolipid content of the plasma membrane releases the eisosome components Slm1/2, which then associate with the TORC2 complex. At TORC2 the Slm1/2 proteins aid in the regulation of the kinase Ypk1, which in turn regulates endocytosis and sphingolipid synthesis. This role of eisosomes in stress response is similar to functions identified for the mammalian caveolae (Sinha *et al.*, 2011), suggesting that these two plasma membrane lipid domains might represent analogous structures.

The localization of the Can1 (Malinska *et al.*, 2003), Tat2 (Grossmann *et al.*, 2007), and Fur4 (Malinsky *et al.*, 2010) to eisosomes suggests that these lipid domains are also involved in some way with nutrient import. Can1, Tat2, and Fur4 belong to the APC transporter family; a class of proteins that imports small nutrients such as amino acids and nucleosides from the environment. In yeast,

This article was published online ahead of print in MBoC in Press (http://www.molbiolcell.org/cgi/doi/10.1091/mbc.E17-11-0691) on June 21, 2018.

*Address correspondence to: Markus Babst (babst@biology.utah.edu).

Abbreviations used: AMPK, AMP-dependent kinase; APC, amino acid-polyamine-organocation; MVB, multivesicular body; SD, synthetic defined; SPS, Ssy1-Ptr3-Ssy5.

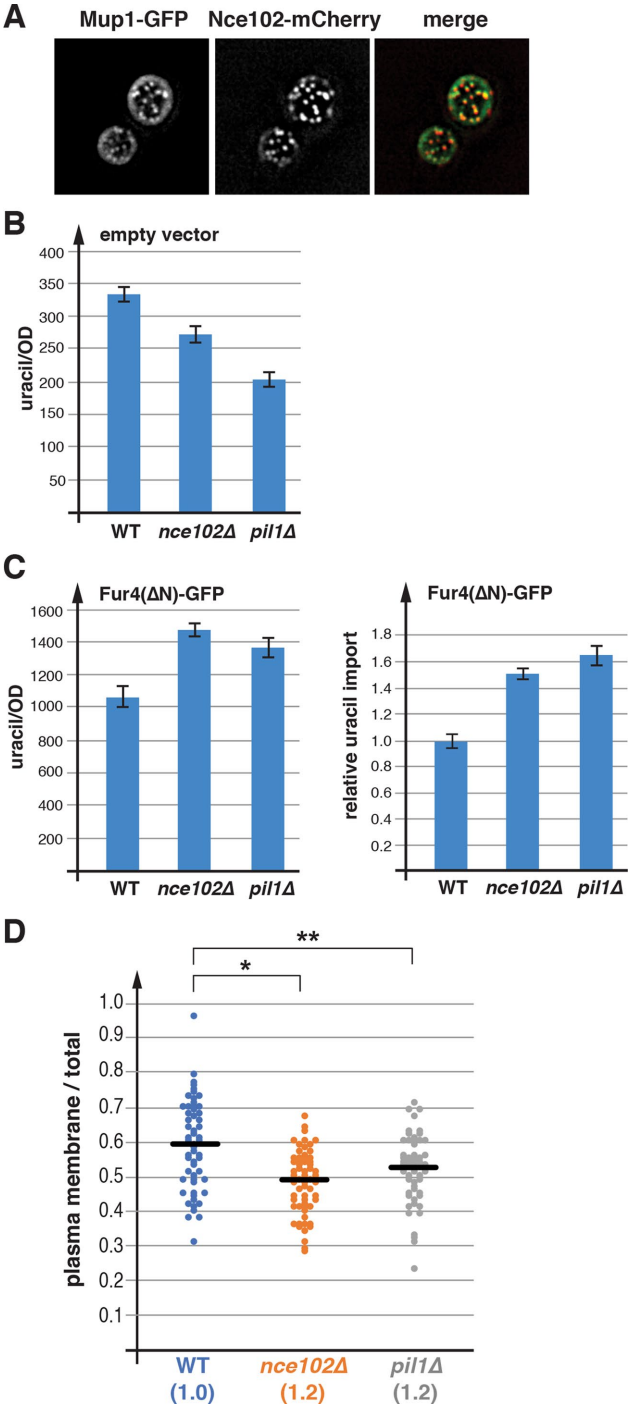


FIGURE 1: Eisosomes are not important for activity but for stability of Fur4. (A) Fluorescence microscopy of yeast expressing the APC transporter Mup1-GFP and the eisosome component Nce102-mCherry (single image of cell surface; strain AMY4 pPL4146 grown in $SD_{comp\text{-}Met}$). (B) Uracil import assays using the strains WT (BY4741), *nce102*Δ (AMY8), and *pil1*Δ (YGR086C). These stains contained an empty plasmid (pRS416) and were grown in $SD_{comp\text{-}ura}$. (C) The same strains containing a plasmid expressing Fur4(ΔN)-GFP (pJK88) were grown in $SD_{comp\text{-}ura}$ and used for uracil-uptake assays. The right panel shows the data standardized by the median GFP fluorescence of these strains (50 cells were quantified by fluorescence microscopy) and by the value of the wild type. (D) Quantitative analysis of fluorescence microscopy pictures of the strains WT (SEY6210 pJK19), *nce102*Δ (AMY41 pJK19), and *pil1*Δ (AMY42 pJK19) grown in $SD_{comp\text{-}ura}$ (~50 cells each). Black lines indicate the median of the data sets. Analysis using *t* test indicated statistically relevant differences between the wild-type and the mutant data set (*, $p = 1.45E\text{-}6$; **, $p = 1.83E\text{-}3$). The numbers in parentheses indicate the Fur4-GFP expression levels relative to wild type (the median of the total fluorescence intensity relative to the wild-type value).

APC transport function is driven by the proton gradient across the plasma membrane. This proton gradient is maintained by the ATP-dependent proton pump Pma1. Therefore, import activity by APC transporters is an ATP-driven process. Other classes of nutrient transporters, such as the structurally related glucose transporters, are not proton driven and do not associate with eisosomes (Spira *et al.*, 2012). Furthermore, Pma1 has been shown to cluster in regions of the plasma membrane that are distinct from eisosomes. Therefore, it has been speculated that it might be functionally important to separate the proton-dependent transporters from the proton pump and this separation is achieved by localizing the transporters to eisosomes (Malinska *et al.*, 2003; Grossmann *et al.*, 2007). It has also been proposed that eisosome localization protects APC transporters from endocytosis, thereby stabilizing these proteins on the plasma membrane (Grossmann *et al.*, 2008). However, a subsequent study questioned the role of eisosomes in transporter stability and showed that APC transporters rapidly exchange between eisosomes and the surrounding membrane (Brach *et al.*, 2011).

Our studies clarify several aspects of eisosome function. The data indicate that eisosomes are storage compartments for APC transporters that can regulate the surface level of these proteins. Eisosomes reduce the substrate-dependent down-regulation of APC transporters and seem to help maintain the plasma membrane proton gradient. Conditions that cause the proton gradient to dissipate, trigger the release of transporters from the eisosome, which aids in the rapid endocytosis and degradation of these proteins. Furthermore, prototrophic growth conditions cause restructuring of eisosomes and rapid removal of APC transporters from the cell surface.

## RESULTS

### Eisosomes stabilize Fur4

The APC transporters Fur4, Tat2, and Can1 have been shown to localize to eisosomes (Malinska *et al.*, 2003; Grossmann *et al.*, 2007; Malinsky *et al.*, 2010). Similarly, we found that the methionine transporter Mup1 localizes at the plasma membrane to eisosomes (Figure 1A). Therefore, it is likely that many of the ~26 APC transporters of yeast are eisosome components. The role of this eisosome association has been controversial. Whereas some studies hypothesized that transporters localizing to eisosomes are active and are protected from endocytosis (Grossmann *et al.*, 2008; Spira *et al.*, 2012), other studies suggested that eisosomes have no effect on stability or activity of the transporters (Grossmann *et al.*, 2007; Brach *et al.*, 2011). To better understand the role of eisosomes, we decided to study their effect on the function of the uracil transporter Fur4.

To determine whether eisosomes influence the activity of Fur4, we performed uracil-uptake assays with wild type and strains deleted for the eisosome components Pil1 or Nce102. Both Pil1 and Nce102 are important components of eisosomes and the lack of these proteins has been shown to cause major disruption of eisosome function, including mislocalization of APC transporters (Grossmann *et al.*, 2008). For the assay, uracil was added to the medium of exponentially growing cells and after 10 min the cells were washed with ice-cold water and extracted with methanol. The

uracil content of these samples was determined by high-pressure liquid chromatography (HPLC; see *Materials and Methods*). We found that uracil import was partially impaired by deleting *PIL1* or *NCE102* (Figure 1B). This import defect could be the consequence of reduced Fur4 activity or decreased levels of Fur4 on the plasma membrane. To differentiate between these two possibilities, we expressed an N-terminally deleted Fur4 that lacks the ubiquitination sites and thus is stabilized at the PM (deletion of amino acid 2-60, referred to as Fur4(ΔN)-GFP [Keener and Babst, 2013]), We found that expressing this form of Fur4 increased the efficiency of uracil import in all three strains by three- to fourfold (import activity of endogenous and Fur4(ΔN)-GFP combined). However, in eisosome mutants intracellular uracil was found to be 50–65% higher relative to wild type (Figure 1C; the right panel shows the uracil import data standardized by the Fur4(ΔN)-GFP expression levels and by the import activity of wild type). This result indicated that eisosomes were not required for Fur4 activity, rather that the presence of eisosomes might partially inhibit import activity. Therefore, the decrease in uracil uptake in *pil1*Δ and *nce102*Δ (not expressing Fur4(ΔN)-GFP) was likely a consequence of Fur4 instability in these strains.

To further test the effect of eisosomes on Fur4 stability, we analyzed fluorescence microscopy pictures of cells expressing Fur4-GFP and determined the ratio of plasma membrane to intracellular GFP signal. Fur4-GFP is endocytosed and delivered via the multivesicular body (MVB) pathway to the lumen of the vacuole for degradation (Blondel *et al.*, 2004; Keener and Babst, 2013). Because GFP degradation is slow, the GFP signal accumulates in the vacuole. Therefore, increased Fur4-GFP degradation causes a decrease in the ratio of cell surface to total GFP signal. It should be noted that not all intracellular GFP signal localizes to vacuoles and thus the ratio of cell surface to total signal is not a direct readout of Fur4-GFP degradation. For the experiments, GFP-tagged Fur4 was expressed from a plasmid, driven by the $Cu^{2+}$-regulated promoter of the *CUP1* gene. The presence of 0.1 mM $Cu^{2+}$ in the medium (used to induce expression) did not affect the growth rate of the yeast cells and had no obvious effect on the localization of Fur4-GFP (Supplemental Figure 1, A and B). Although the *CUP1* promoter–driven expression of Fur4-GFP was higher than expression from the endogenous promoter, the Fur4-GFP levels were lower than those observed with chromosomally integrated *MUP1-GFP*, suggesting that Fur4-GFP expression was not in a nonphysiological range that might affect trafficking of the protein (Supplemental Figure 1C). This statement was further supported by the observation that the plasmid-encoded version of *FUR4-GFP* responded similarly as the chromosomally tagged version in response to proton gradient loss (Supplemental Figure 1D).

Quantitative analysis indicated that deletion of *PIL1* or *NCE102* caused a small but statistically significant drop of Fur4-GFP signal at the plasma membrane, consistent with the predicted increase in Fur4 turnover in eisosome mutants (Figure 1D). Together, our data supported the model that eisosomes function in stabilizing APC transporters at the plasma membrane, possibly by interfering with Rsp5-mediated ubiquitination. In addition, eisosomes seem to impair the import activity of transporters. However, the observed effects were rather small, which might explain the contradicting conclusions of several previous eisosome studies (Grossmann *et al.*, 2007, 2008; Brach *et al.*, 2011; Spira *et al.*, 2012).

### Substrate causes APC transporters to move out of eisosomes

Previous studies reported that in the presence of high substrate concentrations, nutrient transporters such as Tat2 and Can1 move out of eisosomes and redistribute to the surrounding lipid domain, although the effect of substrate on the eisosome association of Can1 is controversial (Grossmann *et al.*, 2008; Brach *et al.*, 2011). To test the effect of substrate on the eisosome localization of Fur4, we performed a series of microscopy experiments to optimize the imaging method. Although the localization of APC transporters to eisosomes has been observed in chemically fixed cells as well as in live cells on glass slides, we noticed inconsistencies with data obtained by these methods. Therefore, we decided to use a microfluidics system that would allow us to maintain constant environmental conditions during the observation of live cells (constant growth medium and temperature) and when needed change one particular parameter at a time. Furthermore, microfluidics allowed us to image the same cells before and after change of conditions, eliminating the problems of cell-to-cell variability. Our experiments indicated that the microfluidics system is crucial for eisosome localization studies and that even small changes in the yeast environment (e.g., caused by moving cells into new medium or mounting them on glass slides) affected the outcome of the experiments.

Using the microfluidics system, we tested the effect of the substrate uracil on the localization of the N-terminally deleted Fur4, Fur4(ΔN)-GFP, which lacks the ubiquitination sites and thus is not down-regulated by high substrate concentrations or stress conditions. These experiments were performed at 30°C and with continued exchange of growth medium. Our experiments showed that within minutes, the addition of uracil caused the redistribution of Fur4(ΔN)-GFP from eisosomes to the surrounding membrane domain (15 min time point shown in Figure 2A; pictures show projections of 10 images [Z-stack], representing the lower half of the cells). Because Fur4(ΔN) is lacking the Rsp5 targeted Lys-38 and -41, these observations suggested that the movement out of eisosomes is not triggered by ubiquitination and the resulting interactions with the endocytic machinery. Rather, it seems that import activity may drive the redistribution of Fur4 out of eisosomes. In contrast, uracil had no effect on the localization of the eisosome protein Nce102 (Nce102-mCherry; Figure 2A).

In summary, the data indicated that eisosomes stabilize Fur4, partially interfere with Fur4 activity, and release Fur4 in the presence of substrate. These observations fit best to a model in which eisosome-associated Fur4 is in a stable, inactive state. In the presence of substrate, Fur4 moves out of eisosomes to the surrounding membrane domain where it imports uracil and where Rsp5 is able to target Fur4 for ubiquitination and subsequent internalization.

To test whether substrate-dependent redistribution represents a general feature of APC transporters, we analyzed the eisosome localization of the methionine transporter Mup1-GFP. When analyzed in a microfluidics system, we observed that the presence of methionine caused Mup1-GFP to change its localization from eisosomes to a diffuse plasma membrane localization (Figure 2B; pictures show a single image of the yeast surface). Furthermore, after methionine addition bright intracellular structures were observed that most likely corresponded to endosomes (see cross-section of cells in Figure 2B). The appearance of these Mup1-positive endosomes is consistent with the rapid Mup1 endocytosis that has been observed as a consequence of high extracellular methionine concentrations (Menant *et al.*, 2006). These results indicated that similar to Fur4, the presence of substrate causes Mup1 to redistribute from eisosomes to the surrounding membrane domain.

### Eisosomes limit the number of APC transporters at the plasma membrane

The eisosome lipid domain has limited space to store APC transporters. Therefore, we would expect that overexpression of Fur4 might

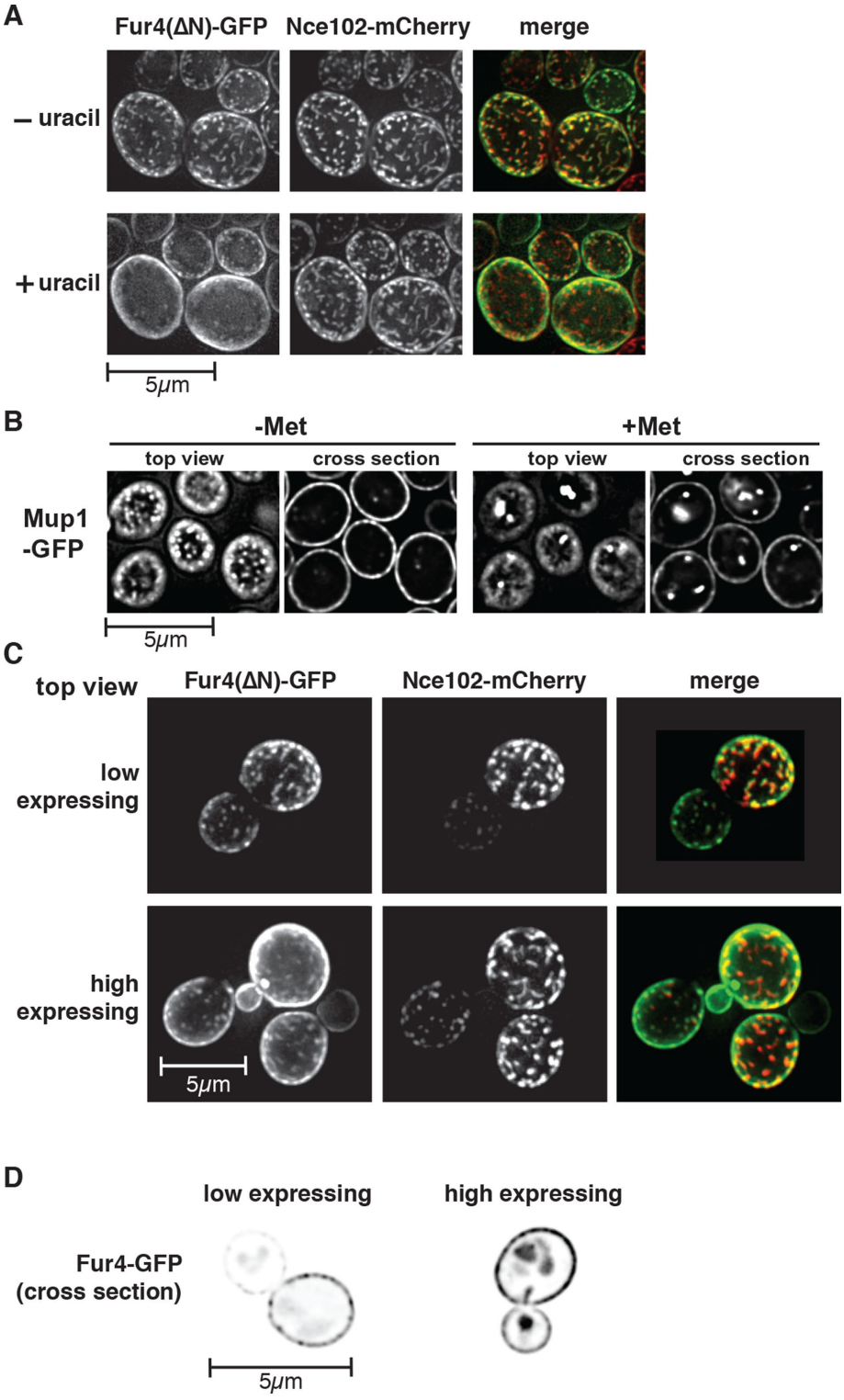


FIGURE 2: Substrate or high expression levels cause APC transporters to accumulate outside of eisosomes. (A) Fluorescence microscopy pictures of wild type expressing Fur4(ΔN)-GFP and Nce102-mCherry (AMY4 pJK30) grown in $SD_{comp\text{-}ura}$ at 30°C in a microfluidics system. The pictures show the projection of 10 optical sections, representing the bottom half of the cell. The cells were switched to $SD_{comp\text{-}ura}$ + uracil (20 μg/ml) and imaged after 15 min. (B) Fluorescence microscopy of wild type expressing Mup1-GFP (BWY3817) grown in either $SD_{comp\text{-}Met}$ at 30°C in a microfluidics system. The cells were imaged before and after 15 min of methionine addition (20 μg/ml). The pictures show a single optical section of the yeast surface. (C) Fluorescence microscopy pictures of wild type containing pAM68 (high-copy plasmid containing *fur4(ΔN)-GFP*). The pictures show projections of 10 images (Z-stack of 2.5 μm; top view) of the cells. The panels show both high expressing and lower expressing cells from the same cultures. (D) Fluorescence microscopy of high and low expressing examples of wild type containing pAM67 (high-copy plasmid containing *FUR4-GFP*). The pictures show a single image through the middle of the cell (image is inverted and the GFP signal is represented in black).

overwhelm the eisosome compartment and cause accumulation of the transporter in the membrane domain outside of eisosomes. We analyzed by fluorescence microscopy the distribution of Fur4(ΔN)-GFP overexpressed in wild-type cells from a high-copy plasmid. These plasmids vary dramatically in copy number from cell to cell and thus the expression levels of Fur4(ΔN)-GFP vary accordingly. We observed that cells with very high expression levels showed a diffuse Fur4 distribution, with less obvious eisosome localization. In contrast, the lower expressing cells in the same culture exhibited obvious eisosome localization (Figure 2C). These observations were consistent with the idea that at high concentration of transporters, the excess of these proteins localizes to the lipid domain outside of eisosomes. In addition, cells overexpressing full-length Fur4-GFP showed increased vacuolar localization of the transporter (increased internal signal; Figure 2D), which supported the model that outside of eisosomes Fur4 has a higher chance to be ubiquitinated and removed from the cell surface. Together these findings suggested that eisosomes might function in limiting the total number of APC transporters at the plasma membrane.

### Modeling of eisosome function

FRAP experiments have indicated that the eisosome localization of APC transporters is dynamic and that these transporters move between eisosomes and the surrounding membrane even in the absence of substrate. Based on this observation, it was concluded to be unlikely that eisosomes protect APC transporters from endocytosis because the rapid movement between the lipid domains will ensure that a pool of these transporters is exposed to the endocytic machinery at all times (Brach *et al.*, 2011). This conclusion is in contrast to our data that suggested a stabilizing effect of eisosomes on Fur4. To shed light on this contradiction, we simulated the dynamic behavior of transporters proposed by Brach *et al.* (2011) with a mathematical model to test whether it is theoretically possible that the proposed dynamic equilibrium can affect transporter

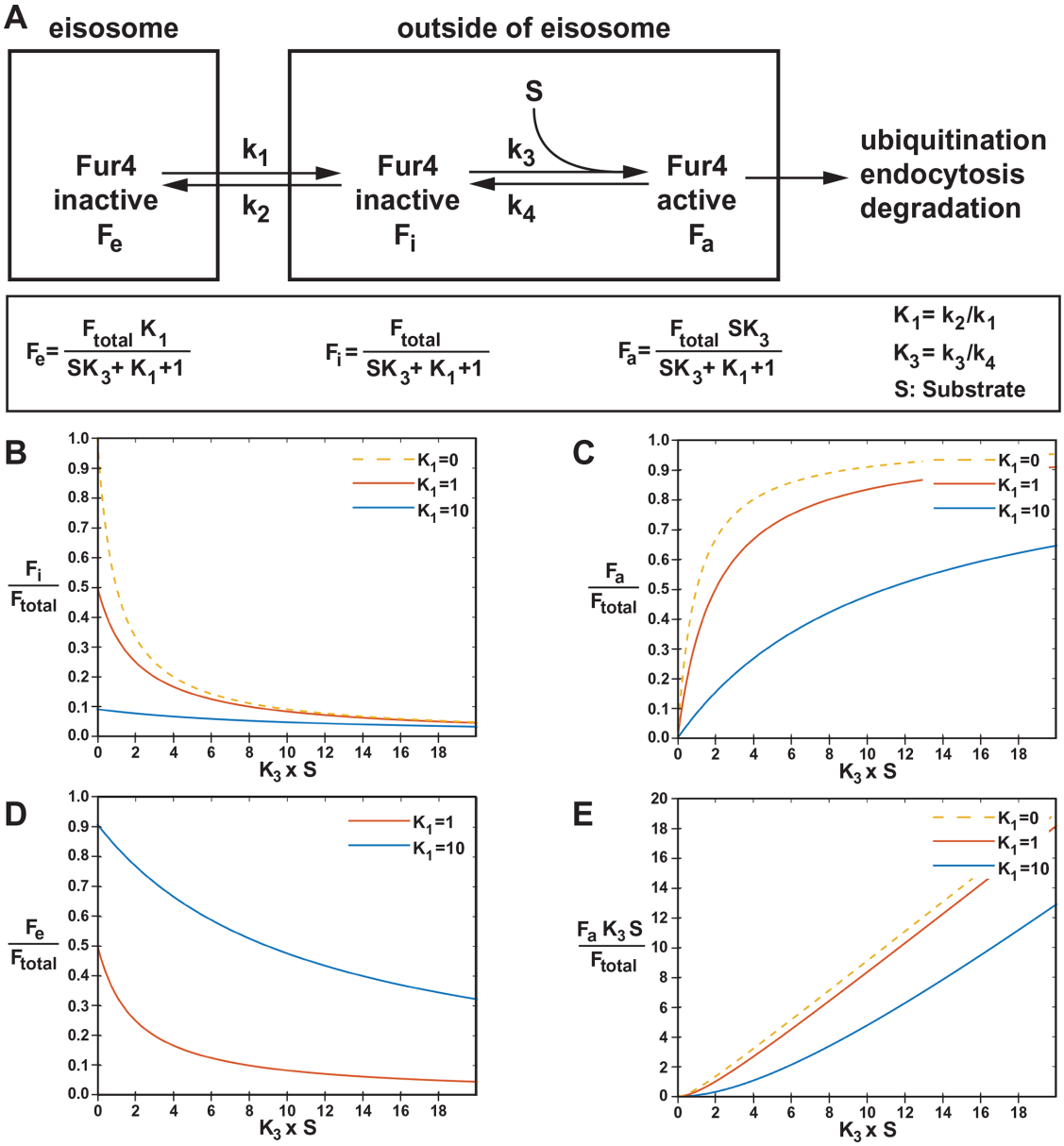


FIGURE 3: Mathematical model of the postulated effect of eisosomes on the stability and function of APC transporters. (A) Model of the eisosome system. Inactive Fur4 (not importing substrate) is in equilibrium between the inside and the outside of eisosomes. Outside of eisosomes inactive Fur4 can encounter substrate (uracil) and become active. Active Fur4 imports the substrate and can be targeted by Rsp5 for ubiquitination and degradation. (B–E) Response of different pools of Fur4 to increasing substrate concentration ($K_3 \times S$) and different $K_1$ values (determines the equilibrium between the inside and the outside of eisosomes; $K_1 = 0$ means lack of eisosomes; $K_1 = 10$ means in the absence of substrate 90% of Fur4 localizes to eisosomes).

stability. The simple assumptions of the model were that Fur4 is in equilibrium between the inactive, protected eisosome pool and the pool outside of the eisosome that is importing substrate and can be targeted for degradation (Figure 3A). The graphs demonstrate effects of different $K_1$ values (defines the equilibrium between inside and outside the eisosome) on the different pools of Fur4. The key graph to answer our question with regard to Fur4 stability is shown in Figure 3C. Because the active form of Fur4 is being targeted for degradation (Keener and Babst, 2013), the $F_a/F_{total}$ values can be interpreted as turnover rates. The graph showed that, compared with an eisosome mutant ($K_1 = 0$), Fur4 is stabilized when in equilibrium with eisosomes. In the case of $K_1 = 10$, in which 90% of inactive Fur4 is eisosome localized, the stabilization effect was rather strong, particularly at lower substrate concentrations (small $K_3S$ values). Furthermore, the graph in Figure 3E indicated that the stabilization effect comes with a price, a reduced import efficiency (lower $F_aK_3S/F_{total}$ values). Together, modeling demonstrates that the fast exchange of transporters between eisosomes and the surrounding membrane does not preclude a stabilization effect of the eisosomes. Furthermore, the predictions from the modeling fit well with our observations that the presence of eisosomes stabilizes Fur4 and partially interferes with import activity (Figure 1).

We tested the prediction that low uracil concentrations should destabilize Fur4 in eisosome mutants to a larger extent than in wild

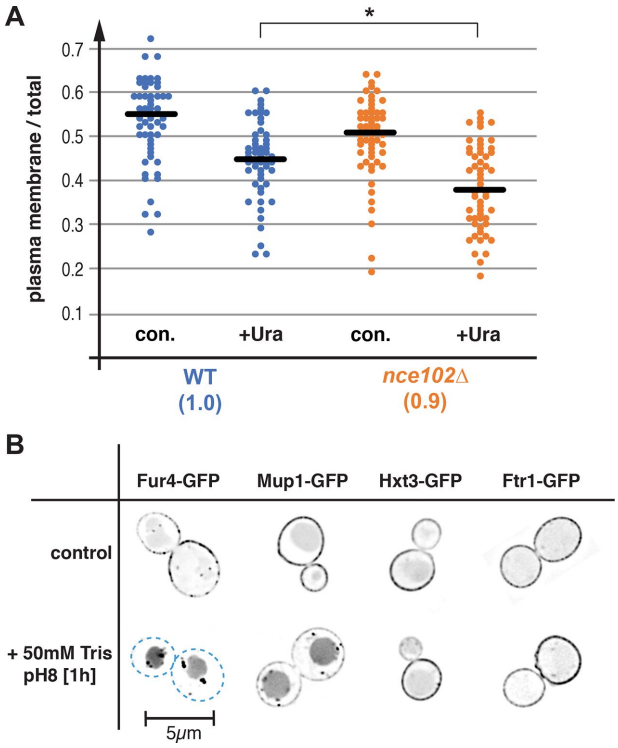


FIGURE 4: Eisosomes protect Fur4 from high down-regulation rates. (A) Quantitative analysis of fluorescence microscopy pictures of wild type and *nce102*Δ expressing Fur4-GFP (SEY6210 pJK19 and AMY41 pJK19) taken before (con.) or after 30 min of uracil treatment (+Ura; 4 μg/ml). Black line indicates the median of the data sets. *t* test indicates that the difference between the wild-type and mutant data set is significant (*, $p = 5.29E\text{-}4$). The numbers in parentheses indicate the Fur4-GFP expression levels in the control cells relative to wild type (the median of the total fluorescence intensity relative to the wild-type value). (B) Yeast strains were grown in $SD_{comp}$ medium to mid–log phase, treated for 1 h as indicated, and analyzed by fluorescence microscopy. The pictures show one optical section from the middle of the cell. The pictures were inverted for better visualization of the GFP signal (GFP signal is shown in black). The following strains were used: Fur4-GFP (SEY6210 pJK19), Mup1-GFP (SEY6210 pMUP1-GFP), Hxt3-GFP (DLY050), and Ftr1-GFP (CBY118). Plasmid-encoded Fur4-GFP and Mup1-GFP behaved similarly to the corresponding chromosomally tagged genes (Supplemental Figure 1A).

type. The quantification of microscopy pictures indicated that compared with wild type, *nce102*Δ showed, in the presence of low concentrations of uracil, increased Fur4-GFP localization to intracellular structures (endosomes, vacuoles; lower plasma membrane/total ratio; Figure 4A). This result fits to the predictions of the mathematic modeling and is consistent with the proposed role of eisosomes in stabilizing APC transporters.

### Loss of the proton gradient causes APC transporters to move out of eisosomes

APC transporter activity is driven by the plasma membrane proton gradient, which is maintained by the proton-pumping ATPase Pma1. The addition of 50 mM Tris (tris[hydroxymethyl]aminomethane), pH 8, buffer to exponentially growing yeast increases the extracellular pH from ~pH 4 (acidified by the growing yeast) to ~pH 7.5, thereby disrupting the plasma membrane proton gradient. We found that this treatment causes rapid endocytosis and vacuolar delivery of the APC transporters Fur4 and Mup1, suggesting that these proteins are rapidly degraded (Figure 4B). In contrast, loss of the proton gradient had no effect on the plasma membrane localization of Ftr1 (iron transporter) or Hxt3 (glucose transporter), two transporters that do not localize to eisosomes (Spira *et al.*, 2012) and are not dependent on the proton gradient (Figure 4B).

Because our data suggested that eisosomes are involved in the regulation of APC transporter surface levels, we tested whether loss of the proton gradient affected the eisosome localization of Fur4. Using the microfluidics system, we observed the redistribution of Fur4(ΔN)-GFP after the addition of Tris buffer. This change of Fur4 localization from eisosomes to the surrounding membrane became obvious after 5–10 min (unpublished data), was strongest after 15 min, and remained at that level of redistribution even after 30 min of high pH treatment (Figure 5A). As a result of the Fur4 redistribution, we observed a ~2.5-fold drop in the number of Fur4-marked eisosomes, whereas Pil1 localization remained unchanged (Figure 5A). Similarly, Mup1-GFP showed, after the addition of Tris buffer, loss of eisosome localization and subsequent endocytosis (appearance of bright endosomal structures; Figure 5B). Together these observations suggested that the lack of a proton gradient caused APC transporters to leave eisosomes, and possibly allowed increased access of Rsp5 to the transporters. Therefore, the loss of eisosome localization at high pH might be part of the stress response that triggers rapid down-regulation of the APC transporters. It should be noted that a previous publication described the effects of loss of the plasma membrane proton gradient on APC transporters (Grossmann *et al.*, 2007). However, the study based its findings on the effects of FCCP, an ionophore that not only disrupts the proton gradient at the plasma membrane but also the proton gradient across the inner mitochondrial membrane. As a consequence, mitochondrial function is disrupted, including ATP production and key metabolic pathways, which confounds the results.

### Loss of the proton gradient causes restructuring of eisosomes

Unlike the treatment with substrate that affected the localization of a specific APC transporter, the redistribution observed at high pH affected both Fur4 and Mup1 (Figure 5). Therefore, the loss of eisosome localization of transporters at high pH is likely the consequence of changes in the eisosome compartment rather than changes to the transporters themselves. Consistent with this idea, we observed that Tris treatment caused redistribution of the tetraspan Nce102 from cell surface puncta (eisosomes) to a diffuse surface localization (Figure 6). In contrast, the soluble, membrane-associated protein Pil1 remained in eisosome structures (Figure 5A). Following the localization of other known eisosome components, we found that the tetraspan protein Sur7 was not affected by Tris treatment, whereas the membrane-associated protein Slm1 redistributed from the eisosome structures to fewer but larger puncta (Figure 6). Studies have shown that under stress conditions Slm1 moves from eisosomes to TORC2 complexes at the plasma membrane (Berchtold *et al.*, 2012), suggesting that the larger Slm1-GFP puncta we observed after Tris treatment might correspond to TORC2 assemblies. Together these results indicated that the collapse of the plasma membrane proton gradient resulted in a partial disassembly of eisosomes, causing redistribution of some eisosome components (APC transporters, Nce102, Slm1) without affecting the eisosome association of other components (Pil1, Sur7).

### Eisosomes are regulated by ATP levels and AMPK

Alkaline stress has been shown to cause a transient drop in cellular ATP levels, which activates the AMP-dependent kinase, AMPK

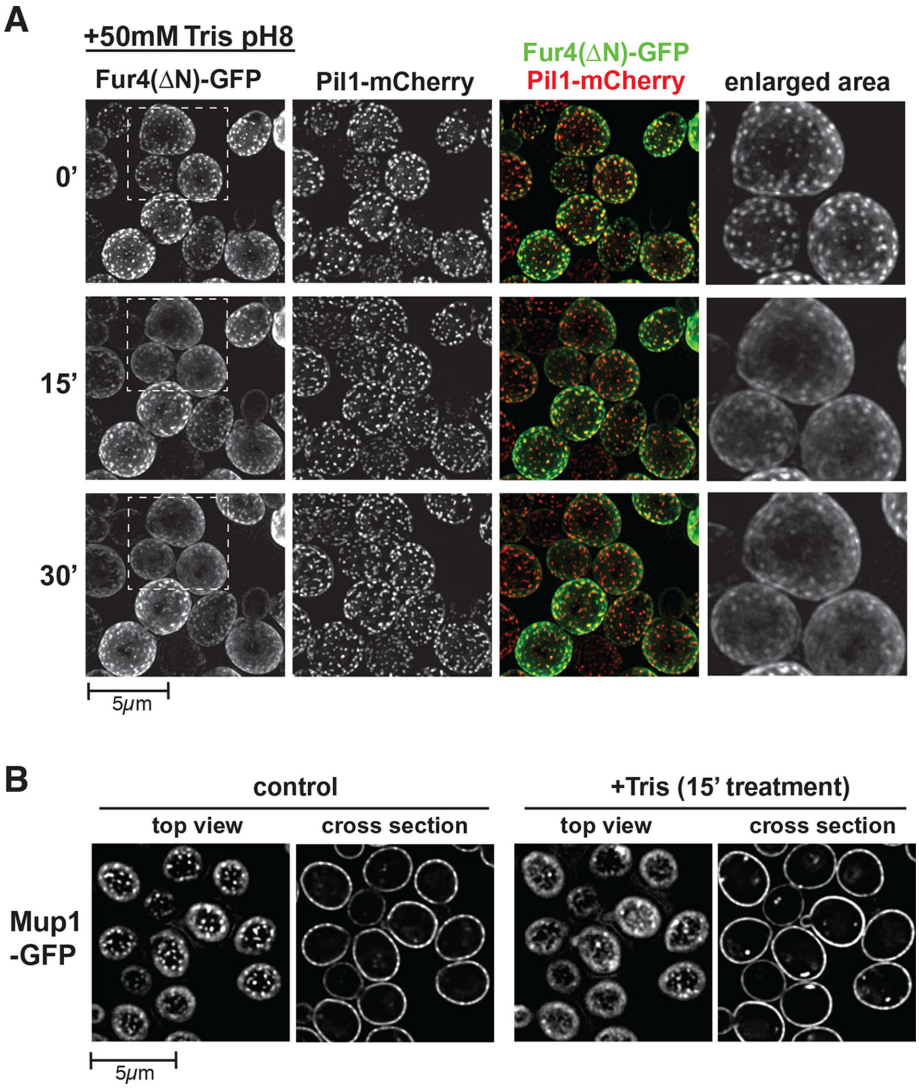


FIGURE 5: Loss of proton gradient causes APC transporter to move out of eisosomes. (A) Fluorescence microscopy of wild type expressing Fur4(ΔN)-GFP and Pil1-mCherry (AMY6 pJK30) grown in $SD_{comp\text{-}ura}$ and imaged using the microfluidics system. Images were taken before ($t = 0$) or after the addition of 50 mM Tris, pH 8, to the growth medium ($t = 15$ min, 30 min). The panels show projections of 10 images (Z-stack, 2.5 μm total), representing the bottom half of the cells. As a consequence of the Tris treatment the number of clearly visible Fur4-labeled eisosomes in the cells of the enlarged area dropped from 95 to 38. (B) The microfluidics system was used to image the eisosome localization of Mup1-GFP in wild-type cells (BWY3817; grown in $SD_{comp\text{-}Met}$) in the presence and absence of 50 mM Tris, pH 8. The pictures show a single image of the cell surface (top view) or of a middle section of the cell (cross-section).

(Chandrashekarappa *et al.*, 2016). Therefore, we determined the effect of Tris addition to the growth medium on the cellular ATP levels by performing in vivo luciferase activity assays. We measured the light emitted from wild-type cells expressing an mCherry-luciferase, a fusion protein optimized for ATP measurements (Rangaraju *et al.*, 2014; mCherry-luciferase localized to the yeast cytoplasm; Supplemental Figure 1E). Light production by luciferase is ATP dependent and thus luciferase assays can be used to determine relative changes in ATP levels. To test the method, we followed cellular ATP levels after addition of $NaN_3$, which caused a rapid initial drop in light emission followed by a partial recovery to ~80% of starting luciferase activity (Figure 7A). Azide blocks mitochondrial ATP production, explaining the initial drop of cellular ATP levels. The observed recovery of luciferase activity most likely reflected an increase in ATP production by glycolysis combined with a reduction in ATP consumption. The combined addition of $NaN_3$ with the glycolysis inhibitor NaF caused light emissions to drop to background levels (levels measured from cells not expressing the luciferase construct; Figure 7B). Together, these results indicated that the luciferase assay is able to measure changes in ATP levels in live yeast. However, these experiments are not internally standardized and thus we are unable to determine the sensitivity or the linear range of the method. Therefore, it is not possible to quantitatively compare different experiments using different treatments.

Using the luciferase assay, we observed that the addition of 50 mM Tris, pH 8 (moves the extracellular pH to ~7.5), caused luciferase activity first to drop rapidly and then to increase to ~140% of the starting value, indicating an increase in cellular ATP concentration after ~2 min at high pH (Figure 7C). These fluctuations in luciferase activity cannot be explained by changes in cytoplasmic pH. Although the cytoplasmic pH slightly increased after Tris addition, the pH remained stable during the time course of the ATP measurements (Figure 7G). Therefore, the likely culprit responsible for these ATP fluctuations is Pma1, the ATP-driven proton pump located at the plasma membrane. Pma1 is one of the most abundant proteins and one of the largest energy consumers in yeast (Morsomme *et al.*, 2000). We predicted that as a consequence of the high extracellular pH, Pma1 activity increased in order to reestablish the proton gradient, which in turn caused the initial drop in ATP levels. The proton gradient is not only required for nutrient uptake but also has important functions for ion homeostasis and osmoregulation. Therefore, maintaining a minimal proton gradient is essential for cell survival (*PMA1* is an essential gene [Serrano *et al.*, 1986]). We propose that in the presence of Tris, pH 8, the ATP consumption of Pma1 reached unsustainably high levels, causing a partial shutdown of Pma1 and the subsequent recovery of ATP levels to values higher than before the treatment.

Because *PMA1* cannot be deleted and specific Pma1 inhibitors are not available, we were not able to directly test whether the observed ATP fluctuations are indeed the consequence of changes in Pma1 activity. However, Pma1 is known to be regulated by Ptk2, a kinase that phosphorylates Pma1 thereby activating the proton pump (Goossens *et al.*, 2000). The Tris, pH 8 treatment of *ptk2*Δ caused a similar initial drop in ATP levels as observed in wild-type cells (Figure 7D). However, following this drop *ptk2*Δ mutants showed a diminished recovery of the ATP levels (reaching ~90% in *ptk2*Δ vs. ~140% in wild type; Figure 7, C and D). This result is consistent with a generally low Pma1 activity in a strain lacking

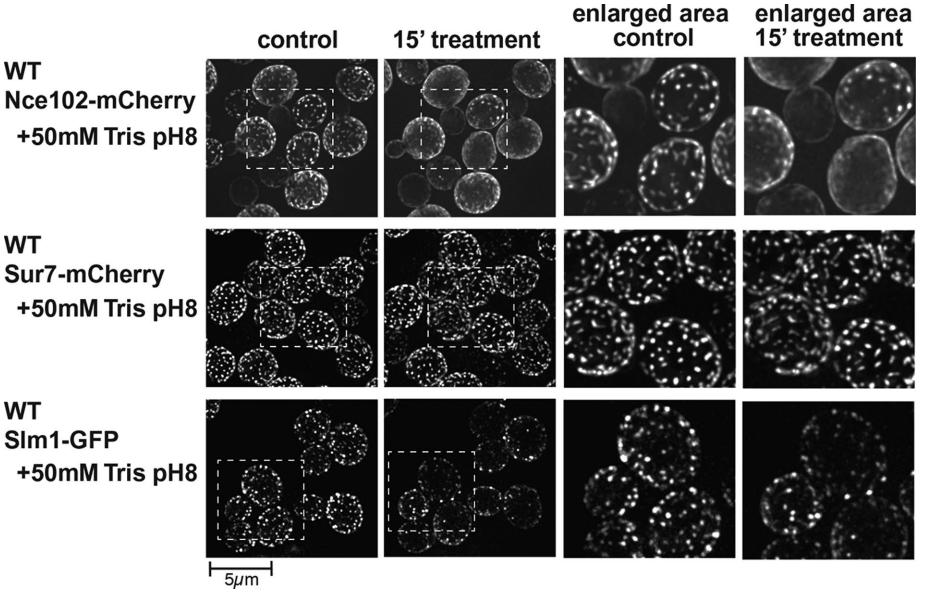


**FIGURE 6:** Alkaline stress causes restructuring of eisosomes. Wild-type cells expressing either Nce102-mCherry (AMY4), Sur7-mCherry (AMY43), or Slm1-GFP (AMY47) were analyzed in the microfluidics system before (control) or after 15-min Tris treatment. The images show the projections of 10 images (Z-stacks of 2.5 μm total).

Ptk2, explaining the lack of a spike in ATP levels after the Pma1 shutdown.

An even more pronounced change in the luciferase activity profile after Tris treatment was observed in an *elo3*Δ strain. *ELO3* encodes a fatty acid elongase that is essential for the synthesis of C26-chain sphingolipids. Deletion of *ELO3* has been shown to affect the stability of Pma1 (Eisenkolb *et al.*, 2002), which suggested reduced Pma1 activity in *elo3*Δ. Consistent with this prediction, we observed a diminished recovery of luciferase activity after Tris, pH 8, treatment (Figure 7F). We propose that the low Pma1 levels in *elo3*Δ do not jeopardize ATP levels after Tris, pH 8, treatment and the cell is able to recover the ATP levels by up-regulating ATP synthesis. Most importantly, the *ptk2*Δ and *elo3*Δ results supported the idea that Pma1 is responsible for the observed ATP fluctuations after Tris treatment.

AMP-dependent kinase (AMPK) is a highly conserved sensor of ATP homeostasis in eukaryotic cells and thus might be involved in the predicted partial shutdown of Pma1 after Tris, pH 8, treatment. Therefore, we analyzed the ATP level changes in a *snf1*Δ strain (deleted for the kinase subunit of AMPK [Ghillebert *et al.*, 2011]) during loss of the proton gradient. The results showed that after the initial drop, AMPK is not required for the recovery of the ATP levels, suggesting AMPK does not regulate Pma1 activity (Figure 7E). However, we found that AMPK is required for the redistribution of APC transporters during proton gradient loss. Microscopic analysis of *snf1*Δ cells in the microfluidics system showed that after Tris treatment both Fur4(ΔN)-GFP and Nce102-mCherry remained in eisosomes in this mutant strain (Figure 8). In contrast, the presence of uracil caused Fur4 to move out of eisosomes even in a strain deleted for *SNF1* (Figure 8), supporting the idea that AMPK regulates the eisosome compartment, whereas substrate (uracil) affects the eisosome localization of a specific transporter.

### APC transporters can secrete nutrients

In vitro studies have indicated that in the absence of a proton gradient, APC transporters lose directionality and thus allow substrates to move across the membrane in both directions (Forrest *et al.*, 2011). This observation suggested that a low proton gradient at the plasma membrane might cause secretion of nutrients from the cytoplasm to the extracellular milieu. We tested this prediction with yeast strains expressing Fur4(ΔN)-GFP. We first treated these growing strains for 10 min with high levels of uracil, then washed the cells with ice-cold water to remove extracellular uracil, and finally incubated the cells in water at 30°C. The transfer of yeast from growth medium into water is well tolerated but will cause acute starvation and thus is predicted to result in partial loss of the proton gradient. Samples were taken at different time points and the intracellular and extracellular uracil concentration was determined by normal-phase chromatography (see uracil-uptake assays in *Materials and Methods*). The data indicated a rapid loss of intracellular uracil (~60% of uracil secreted in 20 min; Figure 7H), supporting the idea that a low proton gradient can cause nutrients to secrete into the extracellular milieu. In contrast, the control sample that remained in ice-cold water for the duration of the experiment showed only minor loss of cellular uracil, indicating that uracil secretion was not due to loss of cell integrity. Similar kinetics of uracil secretion were observed in cells expressing only endogenous Fur4, indicating that the observed uracil secretion was not an artifact of high surface levels of Fur4(ΔN)-GFP (Supplemental Figure 1F). Together, our observations might explain the response of yeast to acute loss of the proton gradient: APC transporters have to be rapidly removed from the cell surface to limit loss of nutrients. Furthermore, the removal of APC transporters from the plasma membrane reduces proton flux and thus helps stabilize the proton gradient.

### Eisosomes are regulated by the metabolic state of the cell

Most APC transporters import amino acids. The expression of these transporters is regulated by the amino acid sensing system referred to as the SPS (Ssy1-Ptr3-Ssy5) sensor (Forsberg and Ljungdahl, 2001). In the presence of extracellular amino acids, the SPS sensor activates transcription factors that increase expression of most amino acid transporters, including Mup1. Therefore, a lack of amino acids in the growth medium is expected to cause a dramatic drop in the levels of APC transporters at the plasma membrane. We tested this prediction by determining the expression levels of Fur4-GFP and Mup1-GFP (GFP-tagged versions of genomic *FUR4* and *MUP1*) in synthetic complete medium ($SD_{comp\text{-}ura}$; contains all amino acids but lacks uracil) versus synthetic medium lacking amino acids ($SD_{-AA\text{-}ura}$). For growth in $SD_{-AA\text{-}ura}$ medium, the strains were converted to prototrophic yeast by introducing plasmids containing the missing biosynthetic genes (*LEU2*, *HIS3*, *LYS2*, *TRP1*, *URA3*). Flow cytometry of these strains confirmed that the expression level of Mup1 is strongly up-regulated in the presence of amino acids (~2.5-fold) compared with the prototrophic medium (Figure 9A). In contrast, the expression of Fur4 showed only a minor change in the different media (Figure 9A). This result was expected because Fur4 is a uracil transporter and thus not under the control of the SPS sensor.

Fluorescence microscopy of cells grown without amino acids indicated that under these conditions most of the Fur4-GFP signal

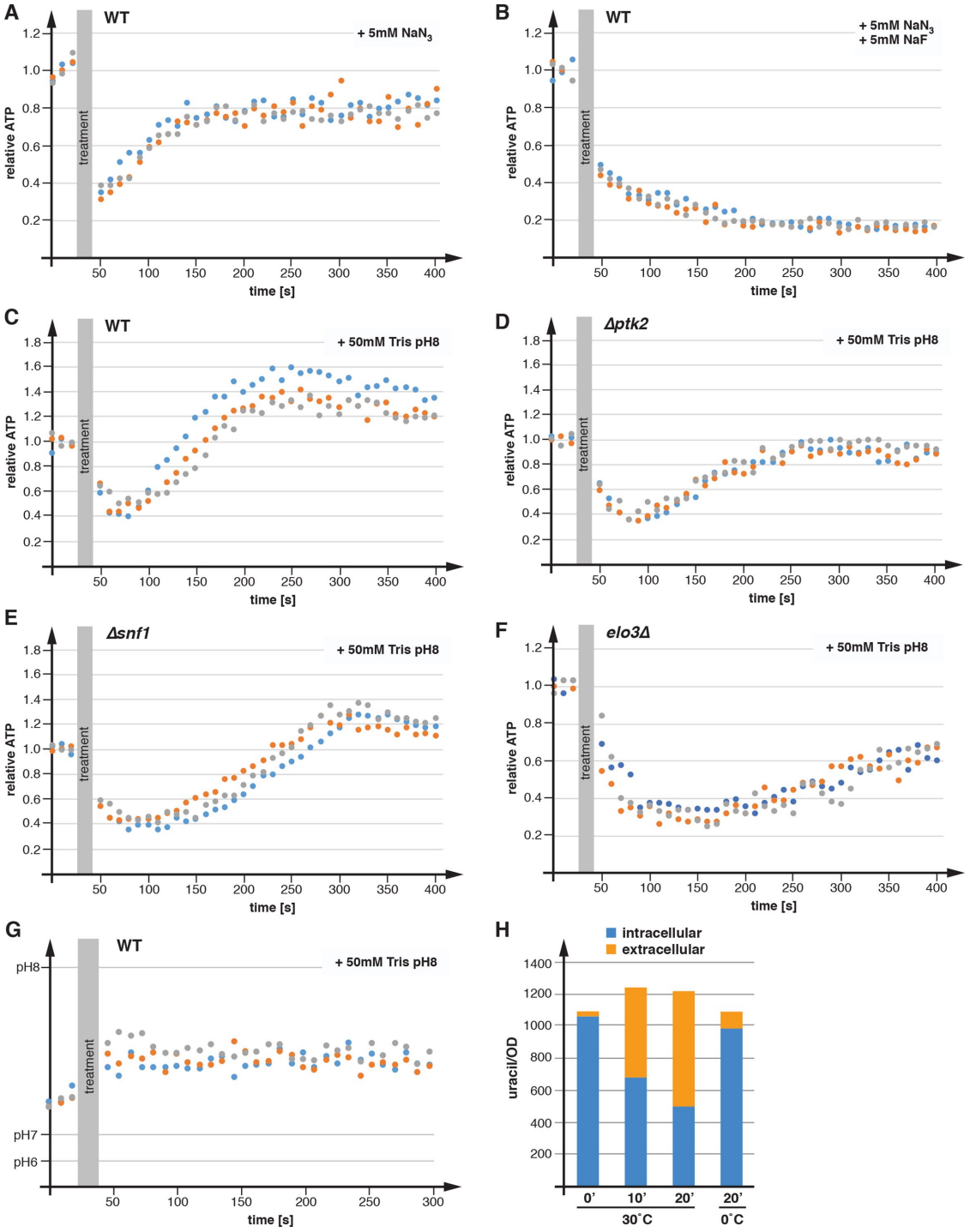


FIGURE 7: Loss of the proton gradient affects cellular ATP levels and causes nutrient secretion. (A–F) The cellular ATP levels of cells grown in $SD_{comp\text{-}ura}$ medium were determined by a luciferase assay. The values of the luciferase activity were standardized relative to starting conditions. The following strains were used: WT (BY4741 pMB522), *ptk2*Δ (YJR059W pMB522), *snf1*Δ (YDR477W pMB522), and *elo3*Δ (YLR372W pMB522). (G) The fluorescence intensity of wild-type cells expressing cytoplasmic pHluorin-mCherry (BY4741 pMB517) was determined before and after the addition of 50 mM Tris, pH 8. The graph shows the ratio of pHluorin to mCherry signal, relative to pH standards (see *Materials and Methods*). (H) Wild-type cells expressing Fur4(ΔN)-GFP (SEY6210 pJK88) were loaded with uracil, washed with 0°C water, and incubated in water either at 30°C or at 0°C. The uracil content of both the cells and the water was determined by HPLC analysis. The graph shows the average of three measurements. The standard deviations were less than 5% (unpublished data).

was found in vacuolar and endosomal structures, suggesting that the flow cytometry data of these cells represented mainly the internalized pool of transporters that are being degraded (Figure 9C). Furthermore, most of Fur4(ΔN)-GFP no longer localized to eisosomes but instead was found diffusely distributed at the plasma membrane (Figure 9D). In contrast, the cells grown in the presence

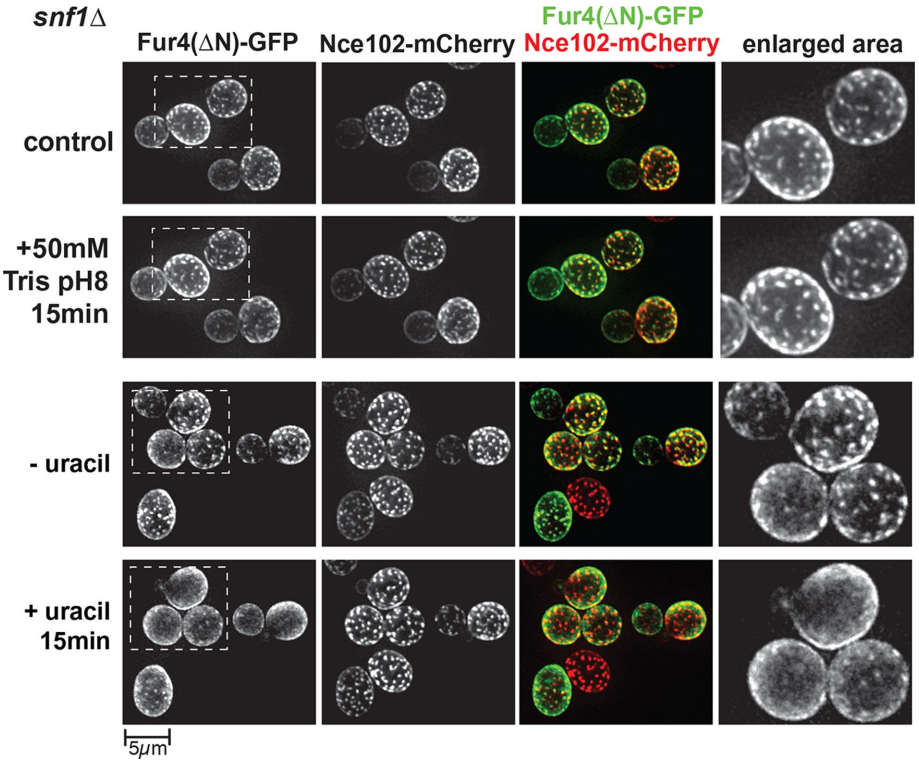


FIGURE 8: AMPK regulates eisosomes. Yeast deleted for the AMPK subunit Snf1, expressing Nce102-mCherry and Fur4(ΔN)-GFP (AMY54 pJK30), were grown in $SD_{comp\text{-}ura}$ and analyzed by fluorescence microscopy using the microfluidics system, before or after the addition of 50 mM Tris, pH 8, or 20 μg/ml uracil. The images show the projections of 10 images (Z-stacks of 2.5 μm total).

of amino acids showed mainly eisosome localization of both Fur4-GFP and Fur4(ΔN)-GFP (Figure 9, C and D).

The microscopy of cells grown in the absence of amino acids also exhibited a change in the eisosome structure. Nce102 was partially delivered to the vacuole, whereas the pool remaining at the plasma membrane localized to fewer but larger/elongated eisosomes (Figure 9, C and D). Together, these observations suggested that growth in the absence of amino acids not only suppressed the expression of amino acid transporters but also caused remodeling of the eisosomes into a membrane domain that inefficiently harbored APC transporters. As a consequence, we observed in $SD_{-AA\text{-}ura}$ medium mainly internal Fur4-GFP signal, which resulted in a ~60% drop in uracil uptake in these cells (Figure 9B).

The APC transporter Gap1 is a broad-specificity, low-affinity amino acid permease that is expressed under poor nitrogen conditions and low extracellular amino acids (Chen and Kaiser, 2002). Consistent with previous findings, we observed a dramatic increase of Gap1-GFP cell surface expression in cells grown without amino acids (see flow cytometry in Figure 9A and microscopy in Figure 9E). Similar to the Fur4-GFP observations (Figure 9D), Gap1-GFP did not localize to eisosome structures in these prototrophic cells (previously observed by Lauwers *et al.* [2007]). However, Gap1-GFP remained at the plasma membrane, indicating that Gap1 stability is not regulated by eisosomes. Together the data supported a model in which the absence of amino acids causes down-regulation of the high-affinity amino acid transporter system together with a loss of eisosome function and replacement of this system with the general amino acid permease Gap1. An interesting aspect of this model is the fact that without extracellular amino acids yeast uses glucose predominantly as a carbon source for amino acid synthesis and less for ATP production, which is the hallmark of the glycolytic metabolism. Therefore, the eisosome–APC transporter system seems to be linked to oxidative phosphorylation, whereas Gap1 functions mainly under a glycolytic/fermentative metabolism.

## DISCUSSION

The eisosome domain is enriched in sphingolipids and ergosterol (Grossmann *et al.*, 2007). These membrane components are known to form less fluid and more ordered lipid environments (Silvius, 2003). The prediction is that the large conformational changes APC transporters undergo during the import cycle (alternative access model of transport [Weyand *et al.*, 2008; Shimamura *et al.*, 2010]) are more restricted in eisosomes than in the surrounding fluid membrane. As a consequence, eisosomes should stabilize APC transporters in their conformational ground state and impair import activity. This prediction fits well with our observations that eisosomes stabilize the cell surface pool of Fur4 but partially impair import activity of the transporter (Figure 1). Together with the finding that the presence of substrate induced the movement of APC transporters out of eisosomes (Figure 2), the data supported the model that APC transporters are in the fluid membrane outside of eisosomes while importing nutrients. In contrast, the localization to eisosomes serves as a storage system for these transporters (Figure 10). Eisosomes solve an inherent problem of APC transporters: on one hand transporters have to be highly flexible in order to undergo the conformational changes necessary for the import activity; on the other hand, structural flexibility makes these transporters susceptible to unfolding and subsequent degradation. By storing inactive APC transporters in eisosomes it is possible to stabilize these proteins and minimize their turnover.

The movement of APC transporters between eisosomes and the surrounding lipid domain has been shown to be highly dynamic (Brach *et al.*, 2011). As a consequence of this dynamic equilibrium, a pool of the transporters is always outside of the eisosomes, even in the absence of substrate. We propose that the conformational changes transporters undergo during nutrient import prevent these proteins from moving back into eisosomes. As a consequence, the presence of substrate traps active transporters outside of eisosomes, thereby shifting the equilibrium in favor of the fluid lipid domain. Therefore, the substrate-induced movement of APC transporters out of eisosomes is simply the result of changing a dynamic equilibrium and does not require an active, lateral transfer of proteins. We incorporated the ideas presented above in a simple mathematical model that describes the behavior of APC transporters as a result of changing substrate concentrations (Figure 3). This model is consistent with the idea that the presence of a storage compartment (eisosome) can, especially at lower substrate concentrations, reduce the degradation rate of the transporters and broaden the dynamic range of nutrient transporter regulation.

Eisosomes also have an important regulatory role by adjusting the number of APC transporters according to the metabolic state of the cell. Unlike other importers such as glucose and iron pumps,

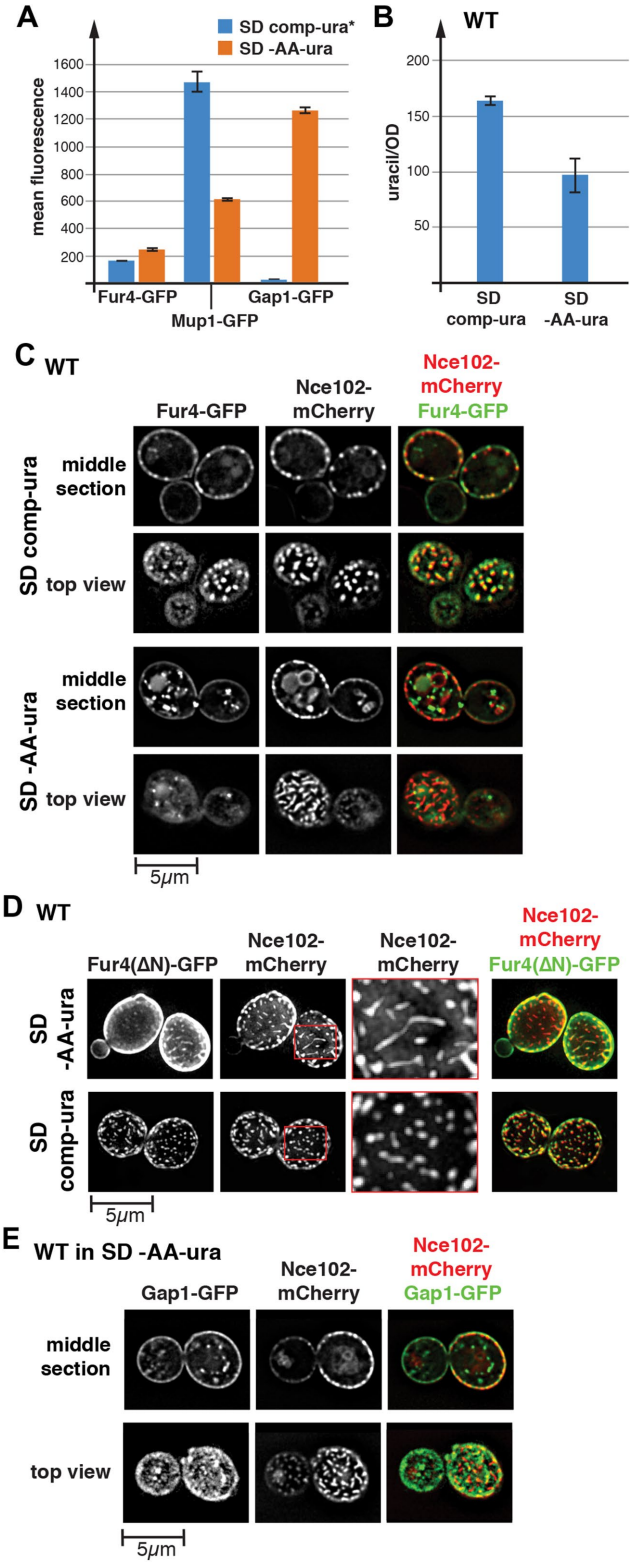


FIGURE 9: Eisosomes of yeast grown without amino acids differ in composition and morphology. (A) Flow cytometry analysis of wild-type cells expressing Fur4-GFP (BWY3815 pRS416), Mup1-GFP (BWY3817 pRS416), or Gap1-GFP (EOY18 pRS416). The cells were grown either in complete synthetic medium ($SD_{comp\text{-}ura}$) or in medium without amino acids ($SD_{-AA\text{-}ura}$). The asterisk indicates that in the case of the Mup1-GFP–expressing strain methionine was not present in the growth medium. For growth in $SD_{-AA\text{-}ura}$, the cells contained plasmids to cover auxotrophic markers (pRS416, pRS413, pRS415, pRS414, and pRS317). The data show the average of three cultures (150,000 events each; fluorescence of a strain not expressing GFP was used for background correction). (B) Uracil import assays of wild-type cells grown either in $SD_{comp\text{-}ura}$ (strain: SEY610 pRS416) or in $SD_{-AA\text{-}ura}$ (strain: SEY6210 pRS413 pRS416 pRS415 pRS414 pRS317). The graph shows the average and SD of three experiments. (C) Fluorescence microscopy of wild type expressing Fur4-GFP and Nce102-mCherry grown either in $SD_{comp\text{-}ura}$ (AMY4 pJK19) or in $SD_{-AA\text{-}ura}$ (AMY4 pJK19 pRS413 pRS415 pRS414 pRS317). (D) Fluorescence microscopy of wild-type cells expressing Fur4(ΔN)-GFP and Nce102-mCherry (AMY4 pJK19 pRS413 pRS415 pRS414 pRS317) grown in $SD_{comp\text{-}ura}$ or in $SD_{-AA\text{-}ura}$ medium. The pictures show a projection of 10 images representing the bottom half of the cell (2.5 μm). The red framed panel shows an enlarged image of the area in the red box. (E) Wild-type cells expressing Gap1-GFP (EOY18 pRS413 pRS416 pRS415 pRS414 pRS317) were grown in $SD_{-AA\text{-}ura}$ and analyzed by fluorescence microscopy.

APC transporters are proton symporters and thus require the proton gradient for import activity. The proton gradient required to maintain this import activity is produced by the proton pump Pma1, one of the largest ATP consumers in yeast (Cyert and Philpott, 2013). The transient drop in ATP levels caused by the disruption of the proton gradient activates AMPK (Chandrashekarappa *et al.*, 2016) and seems to trigger a partial shutdown of Pma1 aimed at restoring the ATP levels. Active AMPK seems to cause the release of APC transporters from eisosomes, which allows for efficient ubiquitination and subsequent delivery to the vacuole for degradation of the transporters (Figure 10). A likely function of this endocytic response is to restore the balance between Pma1 activity (which is low after the shutdown) and the proton fluxing APC transporters (which are numerous). This regulation would ensure that the cytoplasmic pH is maintained and the proton gradient across the plasma membrane is able to recover (the proton gradient is important to maintain ion homeostasis). For the same reason, the eisosome system limits the numbers of APC transporters at the plasma membrane by having limited storage capacity for inactive transporters. We found that overexpression of Fur4 caused a large pool of the protein to localize outside of eisosomes and to vacuoles, suggesting an increase in turnover (Figure 2). Therefore, by regulating eisosome capacity the cell is able maintain the balance between Pma1 activity and the main consumers of the proton gradient, the APC transporters.

Loss of the proton gradient (e.g., caused by the addition of Tris buffer) not only affected APC transporters but also caused the dispersion of the eisosome components Nce102 and Slm1 (Figure 6). This restructuring of the eisosomes was dependent on AMPK, suggesting that the eisosome compartment might be a target of AMPK kinase regulation. The major eisosome components Pil1 and Lsp1 have been shown to be regulated by phosphorylation at several sites, although the consequence of some of these phosphorylation events is controversial (stabilizing or destabilizing the eisosome structure; Walther *et al.*, 2007; Luo *et al.*, 2008; Deng *et al.*, 2009; Mascaraque *et al.*, 2013). We propose that high ATP consumption by Pma1 activates AMPK, which might phosphorylate eisosome components such as Pil1. This phosphorylation causes Nce102, Slm1, APC transporters, and possibly other components to leave the eisosomes. Nce102 is important for the eisosome localization of APC transporters (Grossmann *et al.*, 2008), suggesting that during proton gradient loss these transporters move out of the eisosomes as a consequence of Nce102 dispersal (Figure 10). Although this model represents the simplest explanation of our observations, we do not yet have the data that would support a direct role of AMPK on regulating eisosome composition.

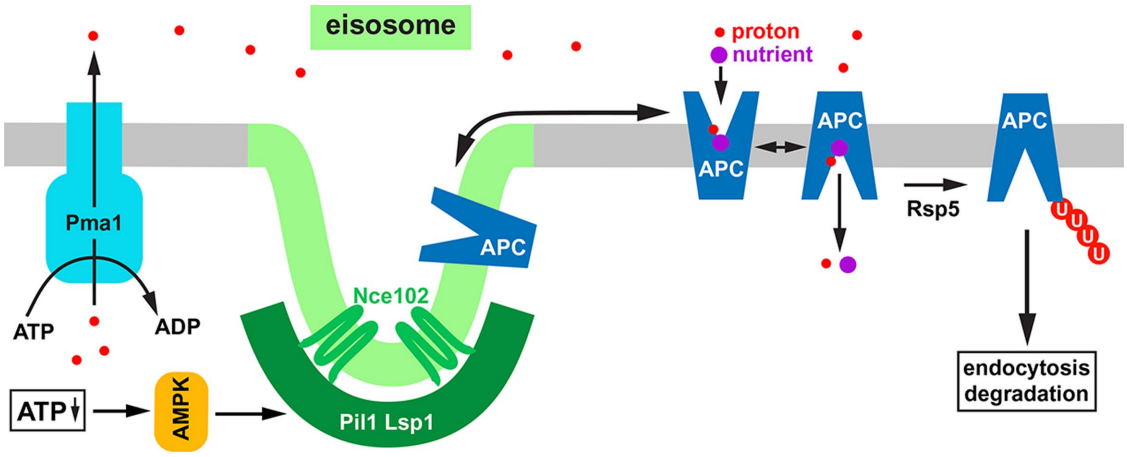


FIGURE 10: Model of eisosome function in yeast. Eisosomes are enriched in sphingolipid/ergosterol (light-green membrane domain), which stabilize APC transporters in an inactive state. APC transporters are moving rapidly between eisosomes and the surrounding fluid phase membrane (gray membrane domain), where these transporters are importing nutrients and can be targeted for ubiquitination by Rsp5. Ubiquitinated APC transporters are endocytosed and degraded in the vacuole. Import activity of APC transporters depends on the proton gradient across the plasma membrane, which is maintained by the ATP-dependent proton pump Pma1. Increased activity of Pma1 (in the case of a reduced proton gradient) causes a drop in cellular ATP levels, which activates AMPK. AMPK targets components of the eisosome (it is not known whether this regulation is direct) and this regulation of eisosomes causes the release of APC transporters and the subsequent exposure of these transporters to Rsp5.

Nce102 is a small, four transmembrane domain–containing protein, also referred to as a tetraspan. Members of this class of protein have been identified in all eukaryotic cells and in almost every organelle. Tetraspans are associated with the formation of membrane microdomains, small assemblies of transmembrane proteins and lipids that function in cell signaling, protein sorting, and cell adhesion (reviewed in Charrin *et al.*, 2014). Tetraspans seem to act as assembly factors that bind to each other, other proteins, and to lipids and thus are able to form within a membrane protein–lipid cluster of defined composition. Consistent with this role, Nce102 and other homologous eisosome proteins might function as assembly factors that cluster sphingolipids and APC transporters and link this cluster to a membrane-associated scaffold, the Pil1-Lsp1 polymer (Figure 10). Therefore, the dispersal of Nce102 observed after proton gradient loss might be indicative of the loss of the protein–lipid microdomain that contained the APC transporters.

Yeast is able to import amino acids or synthesize these essential building blocks using glucose as a carbon source. In the latter case, a large portion of glucose is used anabolically, which is the hallmark of a glycolytic/fermentative metabolism. We found that in yeast grown in the absence of amino acids, Fur4 did not efficiently localize to eisosomes, resulting in delivery of this transporter to the vacuole (Figure 9). Furthermore, these cells exhibited changes of the eisosome structure, which appeared elongated and reduced in numbers. These morphological changes were accompanied by vacuolar localization of a Nce102 pool, suggesting increased degradation of this tetraspan. Together, these observations suggested that eisosome and APC transporter functions are reduced during the glycolytic metabolism, the metabolism that focuses on amino acid synthesis and thus does not require the APC transport system for nutrient import. An exception to this rule is the general amino acid permease Gap1, which is not expressed in the presence of extracellular amino acids but instead is highly induced during prototrophic growth. Therefore, Gap1 seems to be the APC transporter that is not regulated by eisosomes and replaces all the high-affinity amino acid transporters during glycolytic/fermentative growth. Yeast might keep this specialized APC transporter on the cell surface in case nutrient conditions improve and amino acids again become available.

In summary, our study indicated a close relationship between APC transporters and eisosomes. Eisosomes seem to provide a lipid environment that structurally stabilizes APC transporters, thereby minimizing the turnover rate of these proteins. By regulating the size of this lipid environment, yeast is able to maintain the balance between the activity of the proton-pumping Pma1 and the proton importing APC transporters. This type of regulation is a good example of the use of lipid domains to control the function of a whole protein family. The fact that eisosomes change structurally in concert with changes in APC transporter activity suggests that regulating APC transporters is a major function for eisosomes.

## MATERIALS AND METHODS

### Strains, media, and plasmids

The strains (*S. cerevisiae*) and plasmids used in this study are listed in Table 1. For genomic tagging and deletion, homologous recombination was used as described previously (Longtine *et al.*, 1998). KANMX, TRPMX, or HISMX cassettes (or a combination) were used for deletion or tagging of genes. The genetic modifications of strains was confirmed by PCR. For growth of yeast strains, either YPD (yeast extract, peptone, and 2% dextrose) or synthetic dextrose (SD) medium (yeast nitrogen base, 2% glucose) either with amino acids ($SD_{comp}$, in mg/l: *p*-aminobenzoic acid [7.5], Ala [75], Arg [75], Asp [75], Asn [75], Cys [75], Glu [75], Gln [75], His [75], Ile [75], Leu [376], Lys [75], Met [75], Phe [75], Pro [75], Ser [75], Thr [75], Trp [75], Tyr [75], Val [75], adenine [20], inositol [75], and uracil [75]) or without amino acids ($SD_{-AA}$). In cells expressing GFP-tagged versions of Fur4 or Mup1 we removed uracil or methionine from the medium, respectively. Expression of genes under the inducible *CUP1* promoter was induced using 0.1 mM cupric sulfate. Methionine or uracil (20 µg/ml) was used for methionine and uracil treatment, respectively.

| | Descriptive name | Genotype or description | Reference or source |
|---|---|---|---|
| **Strains** | | | |
| SEY6210 | WT | *MATα leu2-3,112 ura3-52 his3-Δ200 trp1-Δ901 lys2-801 suc2-Δ9 GAL* | Robinson *et al.* (1988) |
| BY4741 | WT | *MATa leu2-3112, ura3-52, his3-Δ200* | Winston *et al.* (1995) |
| AMY8 | *nce102Δ* | BY4741, *NCE102:: KANMX6* | This study |
| YLR372W | *elo3Δ* | BY4741, *elo3::KANMX6* | Δ collection strain; Open Biosystems |
| YGR086C | *pil1Δ* | BY4741, *pil1::KANMX6* | Δ collection strain; Open Biosystems |
| CBY118 | *FTR1-GFP* | SEY6210, *FTR1-GFP, HISMX* | Jones *et al.* (2012) |
| DLY050 | *HXT3-GFP* | SEY6210, *HXT3-GFP, KANMX6* | Lang *et al.* (2014) |
| AMY6 | *PIL1-mCherry* | SEY6210, *PIL1-mCherry, KANMX6* | This study |
| AMY4 | *NCE102-mCherry* | SEY6210, *NCE102-mCherry, KANMX6* | This study |
| AMY41 | *nce102Δ* | SEY6210, *NCE102:: KANMX6* | This study |
| AMY42 | *pil1Δ* | SEY6210, *PIL1::KANMX6* | This study |
| AMY43 | *SUR7-mCherry* | SEY6210, *SUR7-mCherry, KANMX6* | This study |
| AMY47 | *SLM1-GFP* | SEY6210, *SLM1-GFP, KANMX6* | This study |
| AMY54 | *snf1Δ NCE102-mCherry* | SEY6210, *SNF1::TRP1, NCE102-mCherry, KANMX6* | This study |
| EOY18 | *GAP1-GFP* | SEY6210, *GAP1-GFP, KANMX6* | This study |
| BWY3815 | *FUR4-GFP* | SEY6210, *FUR4-GFP, KANMX6* | Beverly Wendland |
| BWY3817 | *MUP1-GFP* | SEY6210, *MUP1-GFP, KANMX6* | Prosser *et al.* (2010) |
| **Plasmids** | | | |
| pJK19 | P(*CUP1*)-*FUR4-GFP* | *URA3* (pRS416) P(*CUP1*)-*FUR4-GFP* | Keener and Babst (2013) |
| pJK30 | P(*CUP1*)-*fur4(ΔN)-GFP* | *URA3* (pRS416) P(*CUP1*)-*fur4(Δ2-60)-GFP* | Keener and Babst (2013) |
| PJK88 | P*(SNF7)-fur4(ΔN)-GFP* | *URA3* (pRS416) P(*SNF7*)-*fur4(Δ2-60)-GFP* | This study |
| pPL4146 | P(CUP1)-*MUP1-GFP* | *LEU2* (pRS315) P(CUP1)-*MUP1*-GFP | Stringer and Piper (2011) |
| pMB517 | P(*CUP1*)-sepHluorin-mCherry | *URA3 (pRS416) P(CUP1)*- sepHluorin-mCherry | This study |
| pMB522 | P(*CUP1*)-mCherry-LUCIFERASE | *URA3* (pRS416) P(*CUP1*)-mCherry-*LUCIFERASE* | This study |
| pAM67 | P(*CUP1*)-*FUR4-GFP,* 2μ | *URA3* (pRS426) P(*CUP1*)-*FUR4-GFP* | This study |
| pAM68 | P(*CUP1*)-*fur4(ΔN)-GFP,* 2μ | *URA3* (pRS426) P(*CUP1*)-*fur4(Δ2-60)-GFP* | This study |
| pRS413 | vector | *HIS3(pRS413)* | Christianson *et al.* (1992) |
| pRS414 | vector | *TRP1(pRS414)* | Christianson *et al.* (1992) |
| pRS415 | vector | *LEU2(pRS415)* | Christianson *et al.* (1992) |
| pRS416 | vector | *URA3(pRS416)* | Christianson *et al.* (1992) |
| pRS317 | vector | *LYS2(pRS317)* | Christianson *et al.* (1992) |

**TABLE 1:** Strains and plasmids used in this study.

### Fluorescence microscopy

Fluorescence microscopy was performed on exponentially growing cells ($OD_{600}$ ~ 0.6) using a deconvolution microscope (DeltaVision, GE, Fairfield, CT). For quantitative microscopy analysis, five sections (250 nm step size) through the middle of the cells were imaged, deconvoluted, and collapsed into a single projection. These projections were analyzed using Adobe Photoshop software. The fluorescence intensity outside the cells was set to zero. The "magic wand" tool was used to outline single cells and calculate the total fluorescence value. The outline was contracted by 6 pixels (removes the plasma membrane), and the resulting fluorescence values represented the internal GFP signal. The plasma membrane (total minus internal signal) divided by the total signal is plotted in Figures 1 and 4.

### Microfluidics experiments

For the microfluidics experiments, we used the CellASIC ONIX system (Millipore Sigma) mounted on a deconvolution microscope (DeltaVision, GE, Fairfield, CT). Mid–log phase cells were pumped into the microfluidic chamber. The medium in the chamber was continuously replaced (4 psi pressure). We found that the medium

has to be identical to the growth medium of the cells and cannot be substituted by fresh medium. Therefore, we removed the cells from the growth medium by centrifugation and used this supernatant as the medium for the microfluidics experiments. One key difference between the new medium and the medium of a mid–log phase culture is the pH (new medium = pH 6; mid–log medium = pH 4). For the experiments, the microfluidic chamber was kept at 30°C. Ten images (Z-stacks) were taken at step sizes of 250 nm. These stacked images were deconvoluted and collapsed into single projection (except for Mup1-GFP images where we present only a single image).

### Flow cytometry

Cells grown to mid–log phase were analyzed using the Accuri C6 Flow Cytometer instrument (BD Biosciences). The data of 150,000 events were collected for each sample. Data were collected and analyzed using the CFlow Plus software program. Only events with a forward scattering light (FSC) between 100,000 and 1,400,000 were used for the analysis.

### Uracil-uptake assay

For the import assays, we grew cells in $SD_{comp\text{-}ura}$ medium to mid–log phase, added 20 µg/ml uracil for 10 min at 30°C, and harvested the cells on ice. The cells were washed three times with ice-cold water and extracted at 55°C with 50 µl methanol. The extract was cleared by centrifugation and 5 µl were analyzed by normal-phase chromatography (acetonitrile/water gradient from 100% to 80% in 10 min; Luna-NH2 column; Phenomenex). The presence of uracil was detected by absorption spectroscopy at 260 nm. The measured uracil values were standardized by the optical density of the yeast culture (OD at 600 nm).

### Uracil secretion assay

Cells grown in $SD_{comp\text{-}ura}$ medium to mid–log phase were incubated for 10 min with 20 µg/ml uracil at 30°C, placed on ice, and after 5 min 1 ml of the culture was harvested by centrifugation at 4°C. The cells were washed three times with ice-cold water, resuspended in 100 µl water, and incubated for 0–20 min at 30°C. The samples were centrifuged and supernatant and cell pellets were separated. The supernatant was dried in a SpeedVac and resuspended in 50 µl methanol. The cells were extracted with at 55°C with 50 µl methanol. The supernatant and the cell extract were analyzed by normal-phase chromatography as described above for the uracil-uptake assays.

### ATP measurements

To follow ATP levels, strains were transformed pMB522, a plasmid expressing a luciferase–mCherry fusion protein (optimized luciferase Syn-ATP [Rangaraju *et al*., 2014]). Cells were grown in $SD_{comp\text{-}ura}$ to mid–log phase. MES buffer (10 mM, pH 6) was added for 10 min before ATP measurement. The measurements were performed in a 96-well plate using the Polarstar Optima microplate reader (BMG Labtech). The mid–log phase cells together with 4 mM luciferin were added to the well, and the light emission over time was measured at 30°C.

### Cytosolic pH measurements

Cells expressing pHluorin-mCherry (pMB517) were grown in $SD_{comp\text{-}ura}$ to mid–log phase. The fluorescence intensity of pHluorin and mCherry was measured using the Polarstar Optima microplate reader (BMG Labtech). The ratio of pHluorin to mCherry signal served as a readout for the cytosolic pH. To standardize these measurements, the same cells were measured in the presence of 100 mM buffer solution (MES, pH 6; MES, pH 7; Tris, pH 8) containing 5 mM $NaN_3$, 5 mM NaF, and 10 µM FCCP. All measurements were repeated three times.


## ACKNOWLEDGMENTS

We thank Beverly Wendland (Johns Hopkins University), Mara Duncan (University of Michigan), and Tim Ryan (Cornell University) for sharing strains and plasmids. The research was supported by a grant from the National Institutes of Health (NIH R01 GM123147 to M.B.) and a grant from the National Science Foundation (NSF DMS 1515130 to J.K.).


## REFERENCE


Berchtold D, Piccolis M, Chiaruttini N, Riezman I, Riezman H, Roux A, Walther TC, Loewith R (2012). Plasma membrane stress induces relocalization of Slm proteins and activation of TORC2 to promote sphingolipid synthesis. Nat Cell Biol 14, 542–547.

Blondel MO, Morvan J, Dupre S, Urban-Grimal D, Haguenauer-Tsapis R, Volland C (2004). Direct sorting of the yeast uracil permease to the endosomal system is controlled by uracil binding and Rsp5p-dependent ubiquitylation. Mol Biol Cell 15, 883–895.

Brach T, Specht T, Kaksonen M (2011). Reassessment of the role of plasma membrane domains in the regulation of vesicular traffic in yeast. J Cell Sci 124, 328–337.

Chandrashekarappa DG, McCartney RR, O'Donnell AF, Schmidt MC (2016). The β subunit of yeast AMP-activated protein kinase directs substrate specificity in response to alkaline stress. Cell Signal 28, 1881–1893.

Charrin S, Jouannet S, Boucheix C, Rubinstein E (2014). Tetraspanins at a glance. J Cell Sci 127, 3641–3648.

Chen EJ, Kaiser CA (2002). Amino acids regulate the intracellular trafficking of the general amino acid permease of *Saccharomyces cerevisiae*. Proc Natl Acad Sci USA 99, 14837–14842.

Christianson TW, Sikorski RS, Dante M, Shero JH, Hieter P (1992). Multifunctional yeast high-copy-number shuttle vectors. Gene 110, 119–122.

Cyert MS, Philpott CC (2013). Regulation of cation balance in *Saccharomyces cerevisiae*. Genetics 193, 677–713.

Deng C, Xiong X, Krutchinsky AN (2009). Unifying fluorescence microscopy and mass spectrometry for studying protein complexes in cells. Mol Cell Proteomics 8, 1413–1423.

Douglas LM, Konopka JB (2014). Fungal membrane organization: the eisosome concept. Annu Rev Microbiol 68, 377–393.

Eisenkolb M, Zenzmaier C, Leitner E, Schneiter R (2002). A specific structural requirement for ergosterol in long-chain fatty acid synthesis mutants important for maintaining raft domains in yeast. Mol Biol Cell 13, 4414–4428.

Forrest LR, Kramer R, Ziegler C (2011). The structural basis of secondary active transport mechanisms. Biochim Biophys Acta 1807, 167–188.

Forsberg H, Ljungdahl PO (2001). Genetic and biochemical analysis of the yeast plasma membrane Ssy1p-Ptr3p-Ssy5p sensor of extracellular amino acids. Mol Cell Biol 21, 814–826.

Frohlich F, Moreira K, Aguilar PS, Hubner NC, Mann M, Walter P, Walther TC (2009). A genome-wide screen for genes affecting eisosomes reveals Nce102 function in sphingolipid signaling. J Cell Biol 185, 1227–1242.

Ghillebert R, Swinnen E, Wen J, Vandesteene L, Ramon M, Norga K, Rolland F, Winderickx J (2011). The AMPK/SNF1/SnRK1 fuel gauge and energy regulator: structure, function and regulation. FEBS J 278, 3978–3990.

Goossens A, de La Fuente N, Forment J, Serrano R, Portillo F (2000). Regulation of yeast $H^+$-ATPase by protein kinases belonging to a family dedicated to activation of plasma membrane transporters. Mol Cell Biol 20, 7654–7661.

Grossmann G, Malinsky J, Stahlschmidt W, Loibl M, Weig-Meckl I, Frommer WB, Opekarova M, Tanner W (2008). Plasma membrane microdomains regulate turnover of transport proteins in yeast. J Cell Biol 183, 1075–1088.

Grossmann G, Opekarova M, Malinsky J, Weig-Meckl I, Tanner W (2007). Membrane potential governs lateral segregation of plasma membrane proteins and lipids in yeast. EMBO J 26, 1–8.

Jones CB, Ott EM, Keener JM, Curtiss M, Sandrin V, Babst M (2012). Regulation of membrane protein degradation by starvation-response pathways. Traffic 13, 468–482.

Kamble C, Jain S, Murphy E, Kim K (2011). Requirements of Slm proteins for proper eisosome organization, endocytic trafficking and recycling in the yeast *Saccharomyces cerevisiae*. J Biosci 36, 79–96.
Keener JM, Babst M (2013). Quality control and substrate-dependent downregulation of the nutrient transporter fur4. Traffic 14, 412–427.
Lang MJ, Martinez-Marquez JY, Prosser DC, Ganser LR, Buelto D, Wendland B, Duncan MC (2014). Glucose starvation inhibits autophagy via vacuolar hydrolysis and induces plasma membrane internalization by down-regulating recycling. J Biol Chem 289, 16736–16747.
Lauwers E, Grossmann G, Andre B (2007). Evidence for coupled biogenesis of yeast Gap1 permease and sphingolipids: essential role in transport activity and normal control by ubiquitination. Mol Biol Cell 18, 3068–3080.
Longtine MS, McKenzie A 3rd, Demarini DJ, Shah NG, Wach A, Brachat A, Philippsen P, Pringle JR (1998). Additional modules for versatile and economical PCR-based gene deletion and modification in *Saccharomyces cerevisiae*. Yeast 14, 953–961.
Luo G, Gruhler A, Liu Y, Jensen ON, Dickson RC (2008). The sphingolipid long-chain base-Pkh1/2-Ypk1/2 signaling pathway regulates eisosome assembly and turnover. J Biol Chem 283, 10433–10444.
Malinska K, Malinsky J, Opekarova M, Tanner W (2003). Visualization of protein compartmentation within the plasma membrane of living yeast cells. Mol Biol Cell 14, 4427–4436.
Malinsky J, Opekarova M, Tanner W (2010). The lateral compartmentation of the yeast plasma membrane. Yeast 27, 473–478.
Mascaraque V, Hernaez ML, Jimenez-Sanchez M, Hansen R, Gil C, Martin H, Cid VJ, Molina M (2013). Phosphoproteomic analysis of protein kinase C signaling in *Saccharomyces cerevisiae* reveals Slt2 mitogen-activated protein kinase (MAPK)-dependent phosphorylation of eisosome core components. Mol Cell Proteomics 12, 557–574.
Menant A, Barbey R, Thomas D (2006). Substrate-mediated remodeling of methionine transport by multiple ubiquitin-dependent mechanisms in yeast cells. EMBO J 25, 4436–4447.
Morsomme P, Slayman CW, Goffeau A (2000). Mutagenic study of the structure, function and biogenesis of the yeast plasma membrane $H^+$-ATPase. Biochim Biophys Acta 1469, 133–157.
Prosser DC, Whitworth K, Wendland B (2010). Quantitative analysis of endocytosis with cytoplasmic pHluorin chimeras. Traffic 11, 1141–1150.
Rangaraju V, Calloway N, Ryan TA (2014). Activity-driven local ATP synthesis is required for synaptic function. Cell 156, 825–835.
Robinson JS, Klionsky DJ, Banta LM, Emr SD (1988). Protein sorting in *Saccharomyces cerevisiae*: isolation of mutants defective in the delivery and processing of multiple vacuolar hydrolases. Mol Cell Biol 8, 4936–4948.
Serrano R, Kielland-Brandt MC, Fink GR (1986). Yeast plasma membrane ATPase is essential for growth and has homology with ($Na^+$+ $K^+$), $K^+$- and $Ca^{2+}$-ATPases. Nature 319, 689–693.
Shimamura T, Weyand S, Beckstein O, Rutherford NG, Hadden JM, Sharples D, Sansom MS, Iwata S, Henderson PJ, Cameron AD (2010). Molecular basis of alternating access membrane transport by the sodium-hydantoin transporter Mhp1. Science 328, 470–473.
Silvius JR (2003). Role of cholesterol in lipid raft formation: lessons from lipid model systems. Biochim Biophys Acta 1610, 174–183.
Sinha B, Koster D, Ruez R, Gonnord P, Bastiani M, Abankwa D, Stan RV, Butler-Browne G, Vedie B, Johannes L, *et al.* (2011). Cells respond to mechanical stress by rapid disassembly of caveolae. Cell 144, 402–413.
Spira F, Mueller NS, Beck G, von Olshausen P, Beig J, Wedlich-Soldner R (2012). Patchwork organization of the yeast plasma membrane into numerous coexisting domains. Nat Cell Biol 14, 640–648.
Stringer DK, Piper RC (2011). A single ubiquitin is sufficient for cargo protein entry into MVBs in the absence of ESCRT ubiquitination. J Cell Biol 192, 229–242.
Walther TC, Aguilar PS, Frohlich F, Chu F, Moreira K, Burlingame AL, Walter P (2007). Pkh-kinases control eisosome assembly and organization. EMBO J 26, 4946–4955.
Walther TC, Brickner JH, Aguilar PS, Bernales S, Pantoja C, Walter P (2006). Eisosomes mark static sites of endocytosis. Nature 439, 998–1003.
Weyand S, Shimamura T, Yajima S, Suzuki S, Mirza O, Krusong K, Carpenter EP, Rutherford NG, Hadden JM, O'Reilly J, *et al.* (2008). Structure and molecular mechanism of a nucleobase-cation-symport-1 family transporter. Science 322, 709–713.
Winston F, Dollard C, Ricupero-Hovasse SL (1995). Construction of a set of convenient *Saccharomyces cerevisiae* strains that are isogenic to S288C. Yeast 11, 53–55.